Biochimica et Biophysica Acta 1817 (2012) 1597–1607

Contents lists available at SciVerse ScienceDirect

Biochimica et Biophysica Acta

journal homepage: www.elsevier.com/locate/bbabio

Molecular mechanism for the selective impairment of cancer mitochondrial function by a mitochondrially targeted vitamin E analogue

Sara Rodríguez-Enríquez [a,b], Luz Hernández-Esquivel [a], Alvaro Marín-Hernández [a], Lan-Feng Dong [c], Emmanuel T. Akporiaye [d], Jiri Neuzil [c,e], Stephen J. Ralph [c], Rafael Moreno-Sánchez [a,*]

[a] Instituto Nacional de Cardiología, Departamento de Bioquímica, Tlalpan, México D.F. 14080, Mexico
[b] Instituto Nacional de Cancerología, Laboratorio de Medicina Translacional, Tlalpan, México D.F. 14080, Mexico
[c] School of Medical Science, Griffith Health Institute, Griffith University. Southport, Qld 4222, Australia
[d] Robert W Franz Cancer Research Center, Providence Portland Medical Center, Portland, OR 97213, USA
[e] Institute of Biotechnology, Academy of Sciences of the Czech Republic, 142 20 Prague 4, Czech Republic

ARTICLE INFO

Article history:
Received 14 February 2012
Received in revised form 30 April 2012
Accepted 10 May 2012
Available online 22 May 2012

Keywords:
Mitochondria
Respiratory complex II
Vitamin E analogue
Uncoupling
Tumor cells

ABSTRACT

The effects of α-tocopheryl succinate (α-TOS), α-tocopheryl acetyl ether (α-TEA) and triphenylphosphonium-tagged vitamin E succinate (mitochondrially targeted vitamin E succinate; MitoVES) on energy-related mitochondrial functions were determined in mitochondria isolated from AS-30D hepatoma and rat liver, bovine heart sub-mitochondrial particles (SMPs), and in rodent and human carcinoma cell lines and rat hepatocytes. In isolated mitochondria, MitoVES stimulated basal respiration and ATP hydrolysis, but inhibited net state 3 (ADP-stimulated) respiration and Ca^{2+} uptake, by collapsing the membrane potential at low doses (1–10 μM). Uncoupled mitochondrial respiration and basal respiration of SMPs were inhibited by the three drugs at concentrations at least one order of magnitude higher and with different efficacy: MitoVES > α-TEA > α-TOS. At high doses (>10 μM), the respiratory complex II (CII) was the most sensitive MitoVES target. Acting as an uncoupler at low doses, this agent stimulated total O_2 uptake, collapsed $\Delta\psi_m$, inhibited oxidative phosphorylation and induced ATP depletion in rodent and human cancer cells more potently than in normal rat hepatocytes. These findings revealed that *in situ* tumor mitochondria are preferred targets of the drug, indicating its clinical relevance.

1. Introduction

Mitochondria and the mitochondrial function have recently emerged as attractive alternative targets for cancer therapy. It is now clear that a variety of canonical anti-cancer drugs directly affect the mitochondrial function, in addition to targeting DNA, microtubules or other cellular sites. It is also possibly that specific perturbation of the mitochondrial function has important clinical relevance [1,2]. Increasingly, mitochondria are recognized to play an essential role in tumorigenesis through diverse mechanisms, *e.g.*, mutagenesis by transfer and insertion of mitochondrial DNA (mtDNA) into nuclear DNA, altered expression and mutation of mtDNA-encoded proteins, and mitochondrial ROS-dependent stabilization of HIF-1α a key transcriptional factor that regulates tumorigenesis [3,4]. Mitochondria also seem involved in the maintenance of the malignant phenotype through mechanisms possibly related to ATP production [5,6].

Certain anti-cancer drugs such as cisplatin [7,8] preferentially bind to mtDNA rather than to nuclear DNA. The histone-lacking nature of mtDNA structure facilitates the access of drugs, while limited DNA repair mechanisms in mitochondria enhance its mutation rates and permanent damage induced by various agents, often implicating oxidative stress [6,9]. The development of resistance to cisplatin in many tumor cell lines also appears to be related to mitochondrial alterations [10]. Several clinically used anti-cancer drugs such as adriamycin, apoptolidin, or cisplatin also affect the mitochondrial function by inhibiting the Krebs cycle (in particular 2-oxoglutarate dehydrogenase), the respiratory chain (complexes I to IV, CI–CIV) and/or the phosphorylation system (ATP synthase). In addition, these agents can impair the mitochondrial energy metabolism by inducing an uncoupling effect and inhibition of oxidative phosphorylation following the collapse of the H^+ electrochemical gradient across the inner membrane ($\Delta\psi_m$). As a consequence, stimulation of electron transport and O_2 consumption by the respiratory chain ensue, and these events have been shown to occur in both mitochondria and whole cells from non-tumor and tumor tissues [reviewed in 1].

Abbreviations: CII, respiratory complex II; MitoVES, triphenylphosphonium tagged vitamin E succinate; mtDNA, mitochondrial DNA; 2-OG, 2-oxoglutarate; OxPhos, oxidative phosphorylation; Pyr/Mal, pyruvate + malate; RLM, rat liver mitochondria; SDH, succinate dehydrogenase; SMPs, sub-mitochondrial particles; α-TEA, α-tocopheryl acetyl ether; α-TOS, α-tocopheryl succinate; TPP^+, triphenylphosphonium; VE, vitamin E; TTFA, thenoyltrifluoroacetone

* Corresponding author at: Instituto Nacional de Cardiología, Departamento de Bioquímica, Juan Badiano No. 1, Sección XVI, Tlalpan, México D.F. 14080, Mexico. Tel.: +52 55 5573 2911x1298; fax: +52 55 5573 0994.
E-mail addresses: rafael.moreno@cardiologia.org.mx, morenosanchez@hotmail.com (R. Moreno-Sánchez).

0005-2728/$ – see front matter © 2012 Elsevier B.V. All rights reserved.
doi:10.1016/j.bbabio.2012.05.005

Recently, the ester and ether vitamin E (VE) analogues α-tocopheryl succinate (α-TOS) and α-tocopheryl acetyl ether (α-TEA), and the positively charged triphenylphosphonium (TPP^+)-tagged mitochondrially targeted VE succinate (MitoVES) have emerged as a family of drugs acting on mitochondria with potent anti-cancer activity against several experimental and human carcinoma cells but only marginal, if any, effects on normal cells [11–13]. The molecular basis of apoptosis induced by these agents stems from their interaction with the ubiquinone-binding site of CII to stimulate ROS production [12–14]. VE analogues also act as BH3 mimetic-like compounds, blocking the interaction of the anti-apoptotic Bcl-2 family proteins with their pro-apoptotic counterparts, resulting in cytochrome *c* release and caspase activation [15; reviewed in 4,16].

To further define their mechanisms of action and to elucidate the biochemical basis of their selective toxicity for cancer cells, a thorough evaluation of the effects of the three anti-cancer VE analogues on respiratory rates, generation of electrical membrane potential, Ca^{2+} uptake, as well as ATP synthesis and hydrolysis in mitochondria, sub-mitochondrial particles (SMPs) and cells was undertaken in the present study.

2. Material and methods

2.1. SMPs, mitochondria and cells

Tightly coupled bovine heart SMPs were prepared by sonicating mitochondrial suspensions in the presence of 20 mM succinate [17]. Tightly coupled rat liver and AS-30D hepatoma mitochondria [18,19], the rodent AS-30D hepatoma, the human HeLa (cervix) carcinoma cells [20,21], and rat hepatocytes [22] were obtained as previously described.

2.2. Experimental procedures for determination of energy-dependent mitochondrial functions

Respiration of mitochondria was determined using a Clark-type O_2 electrode in an air-saturated medium containing 120 mM KCl, 20 mM MOPS, 0.5 mM EGTA, 5 mM K-phosphate, pH 7.2 (KMEPi buffer) and the indicated oxidizable substrate at 37 °C. Respiration of SMPs was measured in 250 mM sucrose, 10 mM HEPES, 1 mM EGTA, pH 7.3 (SHE buffer) and the indicated oxidizable substrate at 37 °C. Tumor cells and hepatocytes were incubated in the Krebs–Ringer medium (120 mM NaCl, 5 mM KCl, 1 mM $MgCl_2$, 1 mM KH_2PO_4, 1.4 mM $CaCl_2$, 25 mM HEPES, pH 7.4) at 37 °C for evaluation of cellular respiration supported by endogenous substrates. Respiration of intact cells does not change by adding exogenous mitochondrial substrates such as glutamine, glutamate, malate or succinate in short-term experiments [20].

The O_2 solubility at 2240 m altitude was 400 and 390 ng oxygen atoms *per* ml at 37 °C in the KMEPi and SHE buffers, respectively, and 380 ng oxygen atoms *per* ml at 37 °C in the Krebs–Ringer buffer.

The difference in the electrical potential across the inner mitochondrial membrane ($\Delta\psi_m$) was estimated qualitatively in isolated mitochondria by following the change in absorbance of 5 μM safranin O at 554 *minus* 520 nm in a dual-wavelength spectrophotometer [23] using mitochondria (0.5 mg protein/ml) incubated in the KMEPi buffer at 37 °C. Determination of the pH gradient in SMPs was carried out as described elsewhere [24].

The $\Delta\psi_m$ in intact cells was determined by following the fluorescence changes of rhodamine 6G [25,26]. Cells at 0.5 mg protein/ml were incubated in Krebs–Ringer buffer at 37 °C under smooth stirring with 0.25 μM rhodamine 6G (Sigma-Aldrich, St. Luis, MO, USA). The excitation and emission wavelengths were 480 and 552 nm, respectively.

The rate of ATP hydrolysis in intact mitochondria was determined by following the rate of acidification (scalar H^+ release) with the fluorescence pH-sensitive probe pyranine [27]. The reaction medium contained 120 mM KCl, 5 mM $MgCl_2$, 0.1 mM EGTA, 1 mM HEPES pH 8.0, and 2 μM pyranine. Well-coupled isolated mitochondria (0.75 mg protein/ml) were incubated for 2–5 min in the reaction medium at 37 °C. ATP at 1 mM and oligomycin at 5 μM were added to initiate and stop the reaction, respectively. The excitation and emission wavelengths used were 450 and 507 nm, respectively. The fluorescence signal was calibrated by the addition of a known amount of alkali at the end of the experiment. It was assumed that the stoichiometry of scalar H^+/ATP hydrolyzed is 1 at pH 8 [28] and the rate of ATP hydrolysis was corrected by subtracting the remaining rate of H^+ release in the presence of oligomycin.

The Ca^{2+} uptake was assessed essentially as described previously [29]. Mitochondria (0.78 mg protein/ml) were incubated in 120 mM KCl, 20 mM MOPS pH 7.2, 2 mM Pi at 30 °C with 5 mM succinate, 1 μM rotenone, 100 μM $CaCl_2$, 0.21 mM ADP, 1 μg oligomycin/ml, and 50 μM arsenazo III. The changes in the absorbance difference at 685 *minus* 675 nm were followed in a Shimadzu UV-2501PC dual-wavelength spectrophotometer under continuous gassing with 100% O_2 and gentle stirring.

2.3. Complex I and complex II activities

The CI and CII dehydrogenase activities were determined using SMPs (13–52 μg protein/ml) incubated at 37 °C in the SHE medium with 75–100 μM 2,6-dichlorophenol indophenol. The reaction was started by adding succinate (0.25–2 mM) or NADH (0.1–1 mM) as the CII or CI substrate, respectively. The activity was calculated by measuring the absorbance change at 600 nm and by using the extinction coefficient of 21.3 $mM^{-1}\ cm^{-1}$ for the dye reduction [30]. The CII succinate dehydrogenase activity (SDH) was completely inhibited by malonate. The activities of both succinate–cytochrome *c* oxidoreductase (CII + CIII) and NADH–cytochrome *c* oxidoreductase (CI + CIII) were determined using SMPs (25 μg protein/ml) incubated at 37 °C in 50 mM HEPES, pH 7.2, 1 mM cyanide, and 50 μM cytochrome *c* (from horse heart). The reaction was started by adding succinate (0.25–2 mM) or NADH (0.1–1 mM). The activity was assessed in a dual wavelength spectrophotometer by measuring the reduction of oxidized cytochrome *c* over time from the difference in absorbance at 550 *minus* 540 nm and by using the extinction coefficient of 19.1 $mM^{-1}\ cm^{-1}$ [31]. The CII oxidoreductase activity was fully blocked by malonate (2.5 mM) or antimycin (5–10 μM), whereas the CI oxidoreductase activity was 88% inhibited by 20 μM rotenone.

2.4. ATP determination

The cellular ATP content was determined in cells incubated as described above for respiration. The cell samples were treated with 3% (v/v) perchloric acid and centrifuged; the supernatant was neutralized with 3 M KOH/0.1 M Tris and used for determination of ATP by the standard enzymatic method with hexokinase and glucose-6-phosphate dehydrogenase [32].

For this work three different batches of MitoVES were used. MitoVES, α-TOS and α-TEA were dissolved in 70% ETOH/30% DMSO. No effect of drug vehicle was observed for any of the measured parameters.

3. Results

3.1. Mitochondrial respiratory rates

Addition of low (<1 μM) MitoVES concentrations to rat liver (RLM) or AS-30D hepatoma mitochondria, incubated at 37 °C and pH 7.2 or 6.8 with either Pyr/Mal, 2-OG or succinate (+rotenone) (Fig. 1) did not alter the rates of the pseudo-state 4 (before addition of ADP), state 3 (ADP-stimulated) and state 4 respiration (respiratory

rate reached after added ADP has been exhausted). Addition of α-TOS at concentrations lower than 100 μM did not perturb mitochondrial respiratory rates (data not shown). At 0.3 mM α-TOS and at pH 7.2 with succinate as substrate, respiratory rates of the pseudo-state 4 and net state 3 (state 3 respiration *minus* pseudo-state 4 respiration) were inhibited in AS-30D mitochondria by 40% and 10%, respectively. Similar inhibition occurred with either 2-OG or Pyr/Mal as substrate. In marked contrast, α-TOS in the 0.1–0.3 mM range stimulated pseudo-state 4 respiration by 50–100% and inhibited net state 3 respiration by 20–30% in RLM with succinate or Pyr/Mal at pH 7.2. Results with higher α-TOS concentrations are less reliable because the drug becomes less soluble. At 100 μM, α-TEA inhibited pseudo-state 4 and net state 3 mitochondrial rates in RLM with succinate as substrate, pH 7.2, by 30%. Similar results were observed in mitochondria from hepatoma cells.

On the other hand, MitoVES stimulated pseudo-state 4 and state 4 respiratory rates in the 1–20 μM range in both hepatoma mitochondria and RLM with either oxidizable substrates (Figs. 1, 2A and B). The values of half-maximal stimulatory concentration (SC_{50}) required to accelerate pseudo-state 4 respiration are shown in Table 1. MitoVES levels of 10–20 μM sufficed to reach the maximal stimulation of pseudo-state 4 respiration. With succinate (+rotenone) the SC_{50} value for MitoVES in tumor mitochondria was significantly lower than that required for RLM at pH 7.2, whereas statistically significant differences were not reached at pH 6.8 (Table 1). In both types of mitochondria, α-TEA required higher concentration than MitoVES to stimulate the pseudo-state 4 respiration.

The MitoVES-induced respiratory stimulation was accompanied by decreased ADP/O ratios and decreased respiratory control values (Fig. 1). Therefore, MitoVES acting as an uncoupler (H^+ ionophore) inhibited mitochondrial ATP synthesis (*i.e.*, rate of state 3 respiration × ADP/O ratio, a measure of oxidative phosphorylation, OxPhos) (see Fig. 1). Then, due to the difficulty to calculate ADP/O ratios in the presence of high MitoVES, the rate of net state 3 respiration was determined as a more suitable alternative to assess the MitoVES inhibitory effect on OxPhos and respiratory control ratios (Fig. 2C). Thus, at pH 7.2 or 6.8, succinate-driven OxPhos was more susceptible to MitoVES in both AS-30D and RLM than that driven by Pyr/Mal or 2-OG (Table 2). α-TOS and α-TEA also affected the rate of net state 3 respiration in both types of mitochondria, although at significantly higher concentrations (Table 2).

TTFA is a well-known complex II inhibitor that acts in the ubiquinone binding site [33,34], which is the proposed site for MitoVES action [13]. Therefore, as a control of the MitoVES effect on respiratory complex II, the effect of TTFA on mitochondrial energy-dependent functions was also examined. The succinate-dependent state 3 respiration was potently inhibited by TTFA with IC_{50} values of 0.45 ± 0.19 μM (4) and 0.65 μM (2) in AS-30D and rat liver mitochondria, respectively, and full blockade reached at 10 μM (Fig. S1); state 3 respiration with glutamate *plus* malate was 50% inhibited by TTFA at 2.1 ± 0.5 (3) μM and >25 μM (2) in AS-30D and rat liver mitochondria, respectively. Thus, in contrast to MitoVES, TTFA did not stimulate O_2 uptake but it rather behaved as a respiratory inhibitor at least in the 10–100 μM range (Fig. S1). Similarly to MitoVES, TTFA showed preference for tumor over non-tumor mitochondria.

3.2. Mitochondrial membrane potential ($\Delta\psi_m$)

Agents like CCCP that induce classical mitochondrial uncoupling are detected by their ability to stimulate pseudo state 4 and state 4 respiratory rates and inhibit ATP synthesis after collapsing the $\Delta\psi_m$. To firmly establish the uncoupling behavior of MitoVES in the 1–10 μM range, membrane potential was estimated for both AS-30D and liver mitochondria in the presence of MitoVES.

With the AS-30D mitochondria incubated at pH 6.8 and in the presence of succinate + rotenone, 6.7 μM MitoVES induced collapse of the $\Delta\psi_m$, which slowly recovered to a level slightly lower than the control (in the absence of MitoVES; Fig. 3A). Moreover, the stimulation of ATP synthesis by adding ADP was also clearly affected. In contrast, at pH 6.8, 6.7 μM MitoVES exerted a negligible effect on the $\Delta\psi_m$ generated by RLM (Fig. 3C). At pH 7.2 with 8.1 μM MitoVES (Figs. 3B and D), $\Delta\psi_m$ in hepatoma mitochondria did not recover to

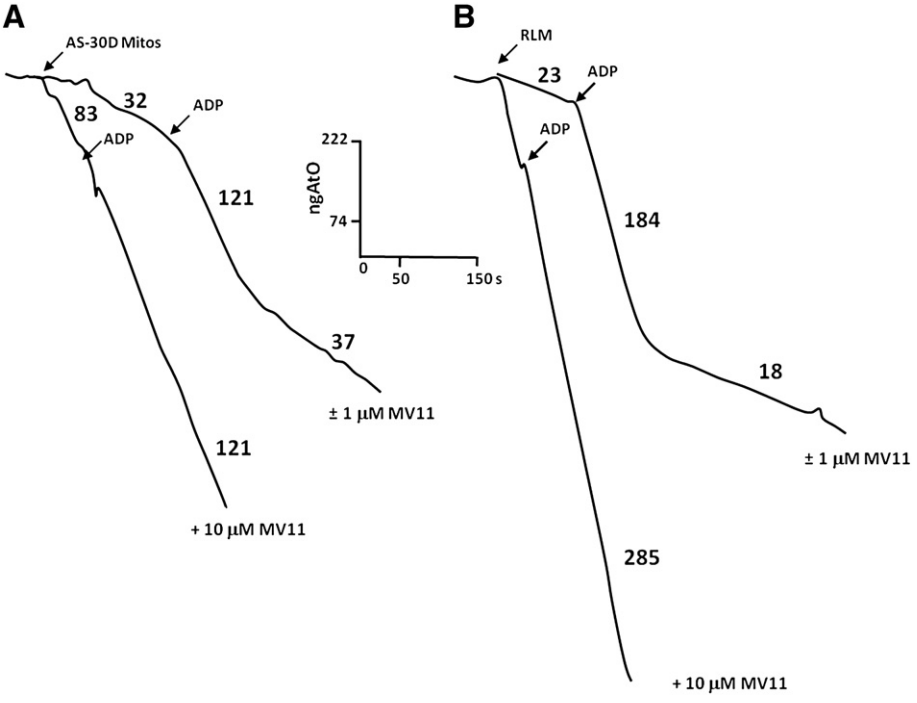

Fig. 1. Effect of MitoVES on respiratory rates of tumor and normal mitochondria. Mitochondria (1 mg protein/ml), isolated from AS-30D hepatoma cells (A) or rat liver (B), were incubated in KME buffer at 37 °C with 10 mM succinate + 1 μM rotenone, 2 mM Pi and the indicated MitoVES (MV11) concentrations. ADP was 200 nmol. The numbers on the traces indicate the rates of O_2 uptake in nanogram atoms oxygen min^{-1} mg $protein^{-1}$ (ngAtO).

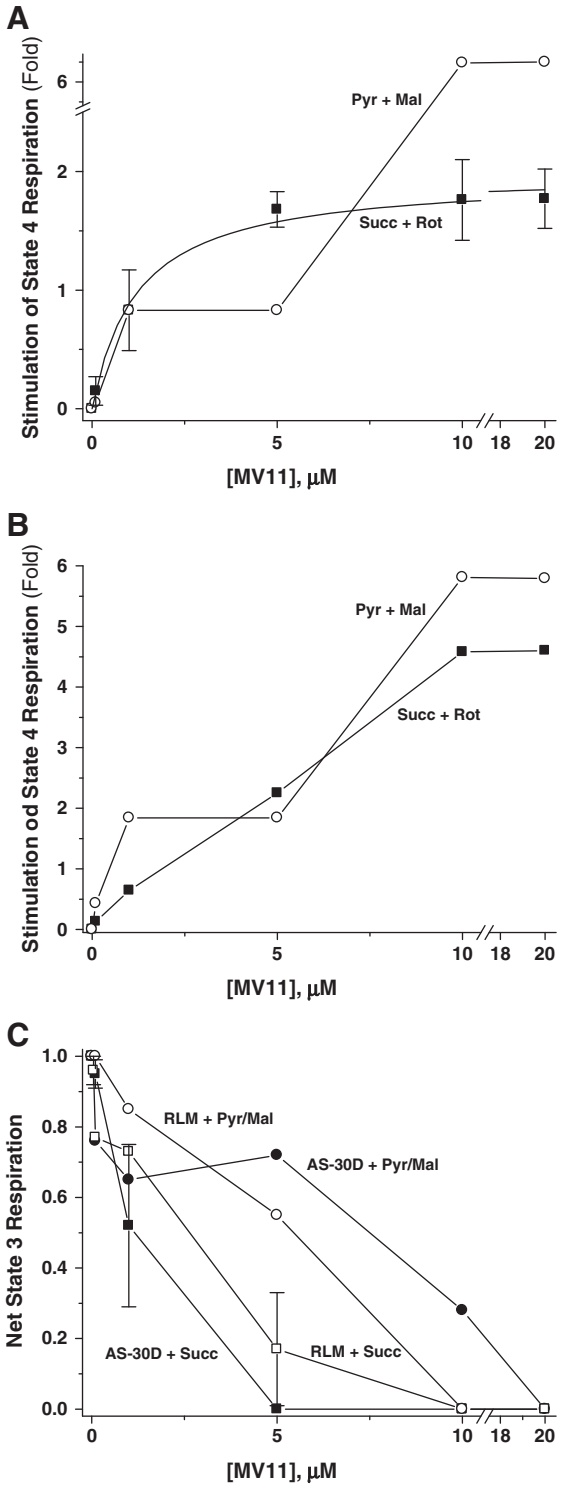

Fig. 2. Effect of MitoVES on mitochondrial respiratory rates. Stimulation of state 4 respiration in hepatoma (A) and rat liver (B) mitochondria. (C) Net state 3 respiration in AS-30D hepatoma and rat liver (RLM) isolated mitochondria with the indicated substrates. The results shown are representative of two–three experiments with similar outcomes, except for those shown with dispersion bars. For clarity, the dispersion bars represent the standard error of the mean.

the control level as it did with the RLM. At 9.4 μM MitoVES, $\Delta\psi_m$ was fully collapsed in hepatoma mitochondria (not shown), whereas liver mitochondria were still able to generate a small $\Delta\psi_m$ signal (Fig. 3C and D). In contrast to the observations with succinate, in both types of mitochondria with Pyr/Mal as substrate 10 μM MitoVES did not induce collapse of the $\Delta\psi_m$, although higher concentrations (≥15 μM) did fully collapse the H^+ gradient (data not shown).

Table 1
Half-maximal stimulatory drug concentrations (μM) of pseudostate 4 respiration in isolated mitochondria.

Substrate	Drug	RLM	Hepatoma	RLM	Hepatoma
		pH 7.2		pH 6.8	
Succ + rote	MitoVES	5.1 ± 2.7 (6)[a,b,c]	1.1 ± 1.1 (3)[a]	12.9 ± 7.6 (4)	2.4 ± 3.7 (3)
	α-TEA	> 100 (3)[b]	198	> 200 (2)	> 150 (1)
	α-TOS	> 300 (3)[c]	> 300 (4)	ND	> 300 (1)
2OG	MitoVES	1.7 (2)	0.9 (2)	9.3 (2)	7.6 (1)
	α-TOS	> 300 (1)	> 300 (3)	ND	ND
Pyr/Mal	MitoVES	13.5 (1)	3.3 ± 2.6 (3)	9.1 (2)	8.5 (2)
	α-TEA	50 (1)	> 200 (1)	> 200 (1)	> 100 (1)
	α-TOS	> 300 (1)	> 300 (1)	> 300 (4)	> 300 (2)

In the absence of drugs, the rates of state 4 respiration (steady-state respiratory rate reached before adding ADP; see Fig. 1) in RLM and hepatoma mitochondria, respectively, with 1–10 mM succinate (Succ) + 1 μM rotenone (rote) at pH 7.2 were 114 ± 43 (n = 9) and 78 ± 47 (n = 5); and at pH 6.8, were 121 ± 30 (n = 5) and 56.5 ± 18 (n = 3); with 10 mM 2OG (+1 mM malate for RLM) at pH 7.2, 45 (n = 2) and 37.5 (n = 2); and at pH 6.8 42 (n = 2) and 36 (n = 1); with 1 mM Pyr + 1 mM (or 0.1–0.3 mM for AS-30D hepatoma) Mal at pH 7.2, 42 (n = 2) and 64 ± 27 (n = 4); and at pH 6.8 37 ± 6 (n = 3) and 62 (n = 2) ngAO/min/mg protein. [a]P < 0.05; [b,c]P < 0.005; Student *t* test for non-paired samples. ND, not determined.

The effect of MitoVES on $\Delta\psi_m$ may be attributed to the inhibition of electron transport rather than to uncoupling. Depending on the concentration, respiratory inhibitors can induce changes in $\Delta\psi_m$ similar to those shown in Fig. 3. Therefore, $\Delta\psi_m$ driven by ATP hydrolysis in isolated mitochondria incubated with increasing MitoVES concentrations was determined to evaluate its possible uncoupling effect on a system not depending on the respiratory chain activity. With 4.7 μM MitoVES and at pH 6.8, the generation of $\Delta\psi_m$ in AS-30D hepatoma mitochondria was severely affected (Fig. 4A), whereas this required 6.75 μM MitoVES before the membrane potential in RLM was similarly depressed (Fig. 4B). TTFA at 10 μM induced a negligible or slight decrease (<15%) in the $\Delta\psi_m$ driven by ATP hydrolysis in RLM and AS-30D mitochondria at pH 7.2 (Fig. S2). At 19 μM, TTFA slowly collapsed the ATP-driven $\Delta\psi_m$ in both types of mitochondria. At 38 μM, TTFA completely collapsed $\Delta\psi_m$ in hepatoma mitochondria, whereas this energy parameter was slowly affected in RLM. For full and rapid collapse of the $\Delta\psi_m$ in RLM, addition of 100 μM TTFA was required (Fig. S2). The collapse of the $\Delta\psi_m$ driven by ATP hydrolysis induced by 10 μM MitoVES was not prevented by 10 μM TTFA (data not shown).

Table 2
Half-maximal inhibitory drug concentrations (μM) of net state 3 respiration in isolated mitochondria.

Substrate	Drug	RLM	Hepatoma	RLM	Hepatoma
		pH 7.2		pH 6.8	
Succ + rote	MitoVES	15.7 ± 4.7 (6)[a]	1.6 ± 1.6 (4)[a,b,c]	13 ± 8 (4)	10.5 ± 5 (3)[d]
	α-TEA	155 (2)	104 (2)	ND	119 ± 52 (3)[d]
	α-TOS		> 300 (4)[c]	ND	> 300 (1)
2OG	MitoVES	12 (2)	9.5 (2)	8.8 (2)	ND
	α-TOS		> 300 (3)	> 200 (4)	ND
Pyr/Mal	MitoVES	8.9 (1)	14.7 ± 5 (3)[b]	15 (2)	12.5 (2)
	α-TEA	113 (1)	> 200 (1)		> 125 (2)
	α-TOS		> 300 (2)	> 200 (3)	> 300 (1)

In the absence of drugs, the rates of net state 3 respiration (state 3 respiration *minus* pseudo-state 4 respiration) in RLM and hepatoma mitochondria, respectively, with 1–10 mM succinate (Succ) + 1 μM rotenone (rote) at pH 7.2 were 340 ± 112 (n = 9) and 78 ± 28.5 (n = 5); and at pH 6.8, were 338 ± 23 (n = 5) and 89 ± 17 (n = 3); with 10 mM 2OG (+1 mM malate for RLM) at pH 7.2, 171.5 (n = 2) and 33 (n = 2); and at pH 6.8 261 (n = 2) and 112 (n = 2); with 1–2 mM Pyr + 1 mM (or 0.1–0.3 mM for AS-30D hepatoma) Mal at pH 7.2, 96 (n = 2) and 164 ± 82 (n = 4); and at pH 6.8, 94 ± 43 (n = 3) and 228 (n = 2) ngAO/min/mg protein. [a,b,c]P < 0.005; [d]P < 0.025; Student *t* test for non-paired samples. ND, not determined.

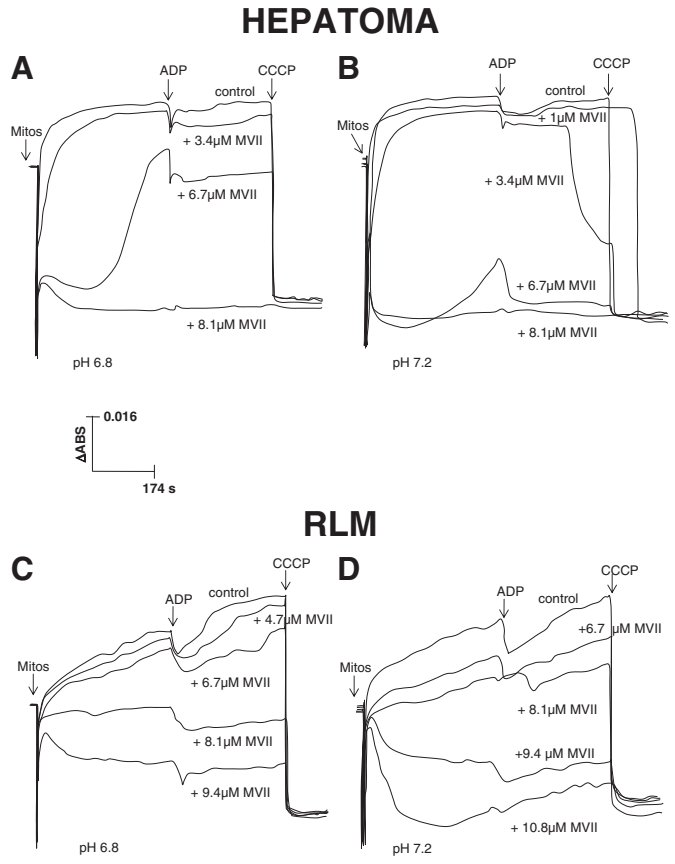

Fig. 3. Effect of MitoVES on membrane potential in rat liver mitochondria (RLM) at pH 6.8 (A) or pH 7.2(C); and AS-30D mitochondria at pH 6.8 (B) or pH 7.2 (D). The traces represent the overlapping of several parallel experiments at different MitoVES concentrations. The incubation medium contained 10 mM succinate + 1 μM rotenone, 5 mM Pi, and the indicated MitoVES (MV11) concentrations. The experiment was started by adding mitochondria (Mitos,0.5 mg protein/ml) and an initial increase in the absorbance difference was observed (generation of membrane potential). A small amount of ADP (600 nmol) was added where indicated to promote ATP synthesis. At the end of all experiments the uncoupler CCCP (4.7 μM) was added to completely collapse membrane potential. The results shown are representative of two independent experiments with similar outcomes.

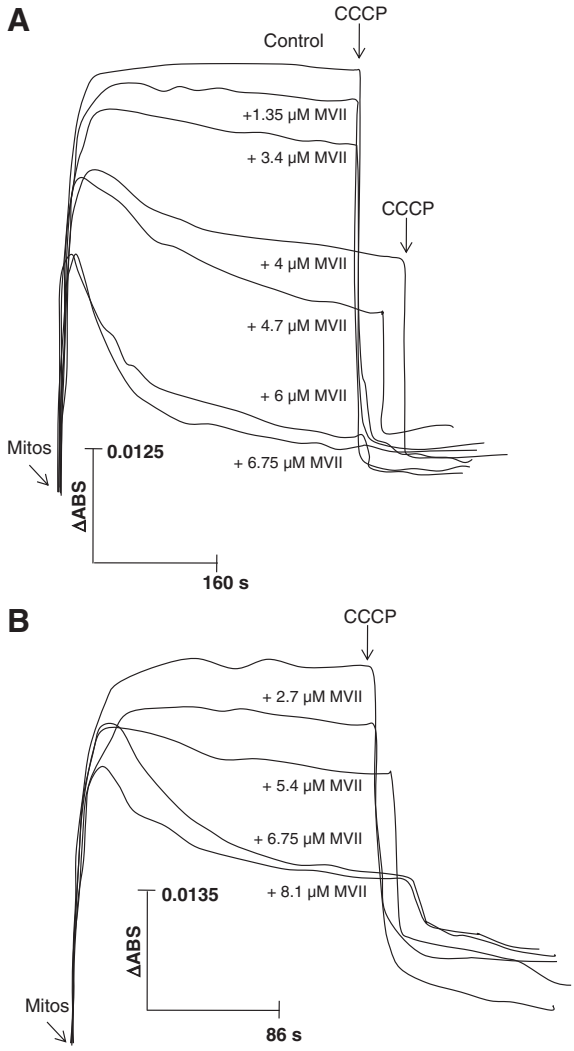

Fig. 4. Effect of MitoVES (MV11) on membrane potential driven by ATP hydrolysis in hepatoma (A) and (B) rat liver mitochondria. The incubation medium contained 0.5 mM KCN and 3 mM ATP and the indicated MV11 concentrations. The experiment was started by adding mitochondria (Mitos, 0.5 mg protein/ml). At the end of all experiments the uncoupler CCCP (4.7 μM) was added to completely collapse membrane potential.

3.3. ATP hydrolysis

The rate of ATP hydrolysis in well-coupled liver (60–106 nmol hydrolyzed ATP/min/mg protein at 37 °C) and AS-30D mitochondria (45 nmol hydrolyzed ATP/min/mg protein at 37 °C) was markedly (25–270%) stimulated by 2–10 μM MitoVES; in turn, CCCP was unable to further stimulated the rate of ATP hydrolysis induced by 10 μM MitoVES. At 15–20 μM MitoVES, the ATP hydrolysis was also stimulated although at a lower extent than that attained at 10 μM. TTFA at 25 μM induced 86% stimulation of ATP hydrolysis in AS-30D mitochondria. These results indicated that MitoVES at 1–10 μM stimulates ATP hydrolysis acting as an uncoupler and does not inhibit the activities of the mitochondrial ATP synthase (catalyzing the reverse reaction as an ATPase) and adenine nucleotide translocase, both required for ATP hydrolysis in intact mitochondria.

3.4. Ca^{2+} release

AS-30D hepatoma mitochondria showed higher capacity for Ca^{2+} uptake than RLM as it has also been reported for Ehrlich ascites mitochondria [35]. The Ca^{2+} uptake by RLM was fully abolished by 20 μM MitoVES (data not shown). In turn, Ca^{2+} release was immediately induced by 2 μM MitoVES or CCCP, or was induced after a short delay at lower doses in both AS-30D and liver mitochondria (Fig. 5). α-TEA in the 30–90 μM range did not promote Ca^{2+} release (data not shown).

3.5. Uncoupled respiration

To examine for the possible inhibitory effect of MitoVES on mitochondrial respiratory enzymes, the rate of uncoupled respiration was determined. In the presence of an excess of an uncoupler, only the inhibitory effect of MitoVES would become apparent, as long as the site of action is localized to the respiratory chain complexes. However, in case of MitoVES targeting the Krebs cycle enzymes, ATP synthase, adenine nucleotide translocase or the P_i carrier, no effect of this agent on uncoupled respiration is anticipated.

The rate of uncoupled respiration (0.5–1 μM CCCP) in AS-30D hepatoma or liver mitochondria was not affected by <10 μM MitoVES or <100 μM α-TOS in 2 or 15 min pre-incubations with succinate (+rotenone) or 2-OG as the oxidizable substrate, and at either pH 7.2 or 6.8 (data not shown). At 100 μM MitoVES, 71–97% inhibition of uncoupled respiration was achieved with succinate or 2-OG as the substrate in both AS-30D or liver mitochondria at pH 7.2. With α-TEA, half-maximal inhibitory concentration (IC_{50}) values of

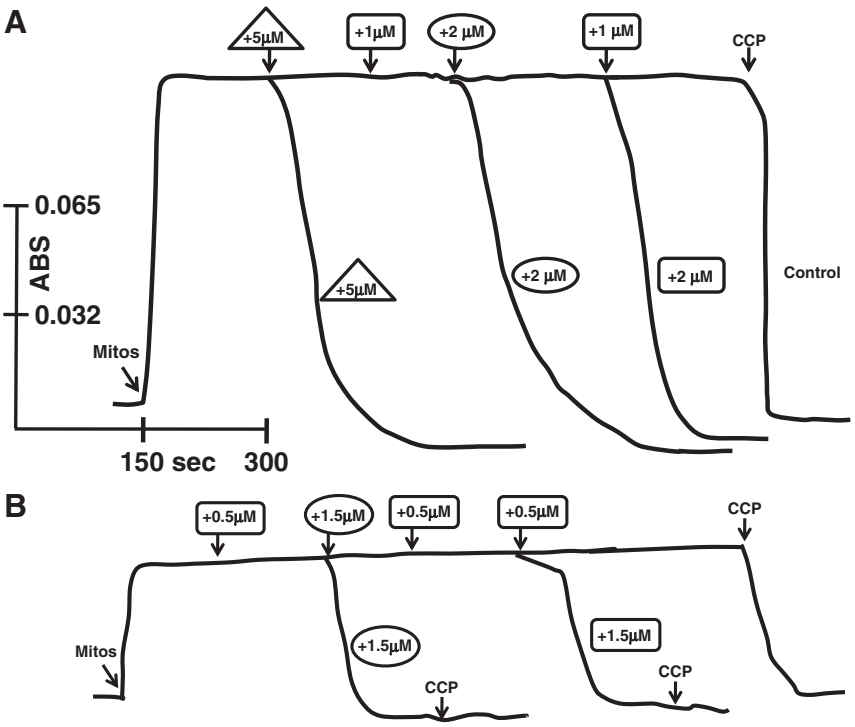

Fig. 5. Effect of MitoVES on Ca^{2+} release in hepatoma (A) and (B) rat liver mitochondria. Traces from different experiments were overlapped. Arrows indicate addition of MitoVES at the concentrations shown on the traces. At the end of all experiments the uncoupler CCCP (CCP, 4 μM) was added to completely collapse the membrane potential. Numbers inside the triangles, circles and squares represent the subsequent addition of variable MitoVES concentrations in different preparations. The experiment shown is representative of three AS-30D and two RLM independent studies with similar results.

50–60 μM (n = 2) and 163 μM were determined for uncoupled respiration in AS-30D and rat liver mitochondria, respectively, incubated with succinate at pH 7.2.

3.6. Respiratory rates in sub-mitochondrial particles

It could be argued that in uncoupled mitochondria MitoVES as a lipophilic cation may not be efficiently accumulated, because no electrical gradient (negative inside) would exist under such conditions, which is required to facilitate localization of the drug at the interface of the inner mitochondrial membrane and the matrix. Therefore, SMPs were prepared to allow for the direct exposure of the respiratory chain complexes to the three different VE analogues. SMPs are inside–out vesicles, in which the matrix side of the inner membrane is exposed to the incubation medium. To assess the orientation and integrity of these vesicles, they were examined for their ability to oxidize NADH (which is not oxidized in intact mitochondria) and to build a pH gradient (which is determined using a permeable amine; in mitochondria, the acidic pH is on the outer side and hence the amine does not permeate). A pH gradient (>1.5) was established in SMPs and the oxidation of NADH was substantial (421–1040 ng atom oxygen min^{-1} mg $protein^{-1}$ at 37 °C and pH 7.4 with 1 mM NADH; with 0.3 mM NADH plus 1 mM $MgCl_2$, activity was 1265 ± 100 ng atom oxygen min^{-1} mg $protein^{-1}$; n = 5), all of which indicated that the SMP preparations consisted of inside–out vesicles.

The IC_{50} values of the respiration rate with succinate as the substrate for MitoVES, α-TEA and α-TOS were 47 ± 7 (n = 3), 37 (n = 2) and 170 μM (n = 2), respectively, whereas for NADH as the substrate they were 30, 30 and 194 ± 18 μM (n = 3), respectively. Addition of Mg^{2+} slightly stimulated the respiratory rates in SMPs (Fig. 6), diminishing the drug potency with succinate or NADH as the oxidizable substrate (>100 μM for MitoVES and α-TEA; and >200 μM for α-TOS), except for MitoVES and NADH (IC_{50} = 28 μM) (Fig. 6). In the experiments where SMPs were pre-incubated with MitoVES or α-TEA for longer periods and with succinate as the substrate, the uncoupling effect of these two drugs became apparent at their lower concentrations (assessed on the basis of stimulation of respiration), while the inhibitory effects on respiration were exerted by these agents at higher concentrations.

3.7. Oxidoreductase and dehydrogenase activities of complexes I and II

In order to further assess the relative efficacies and specificities of MitoVES, α-TEA and α-TOS, the effects of these drugs on the dehydrogenase and oxidoreductase activities of CI and CII were examined using SMPs. MitoVES disrupted the oxidoreductase activity of CII (*i.e.*, electron transfer from CII to CIII) at relatively low doses (IC_{50} of 5–7 μM; Table 3). The addition of Tween 20 diminished the efficacy of the agent (IC_{50} of 23; n = 2; and 39 ± 16 μM; n = 4, for low and high succinate, respectively). In contrast, MitoVES exerted no discernible effect on the oxidoreductase activity of CI (Table 3). Longer-term experiments (15 min) with or without Mg^{2+} did not improve the drug efficacy (data not shown). Similarly, TTFA inhibited CII oxidoreductase activity with an IC_{50} of 12 μM (in the absence of Tween 20), reaching 80% blockade at 75–100 μM (data not shown); CI oxidoreductase activity was not affected by 100 μM TTFA.

α-TEA and α-TOS affected the CII dehydrogenase activity at similar or slightly higher concentrations than those required for its inhibition by MitoVES, whereas the CII oxidoreductase activity was significantly less sensitive. The CII dehydrogenase activity was less sensitive than the oxidoreductase activity to MitoVES, as previously reported [13]. The CI dehydrogenase and oxidoreductase activities were not affected by the three drugs at concentrations below 100 μM (Table 3).

3.8. Cellular respiratory rates, $\Delta\psi_m$ and ATP content

The rate of respiration of the intact hepatoma cells was stimulated by MitoVES in the 1–10 μM range, whereas the sensitivity to oligomycin was decreased at higher concentrations (Figs. 7 and 8). This response

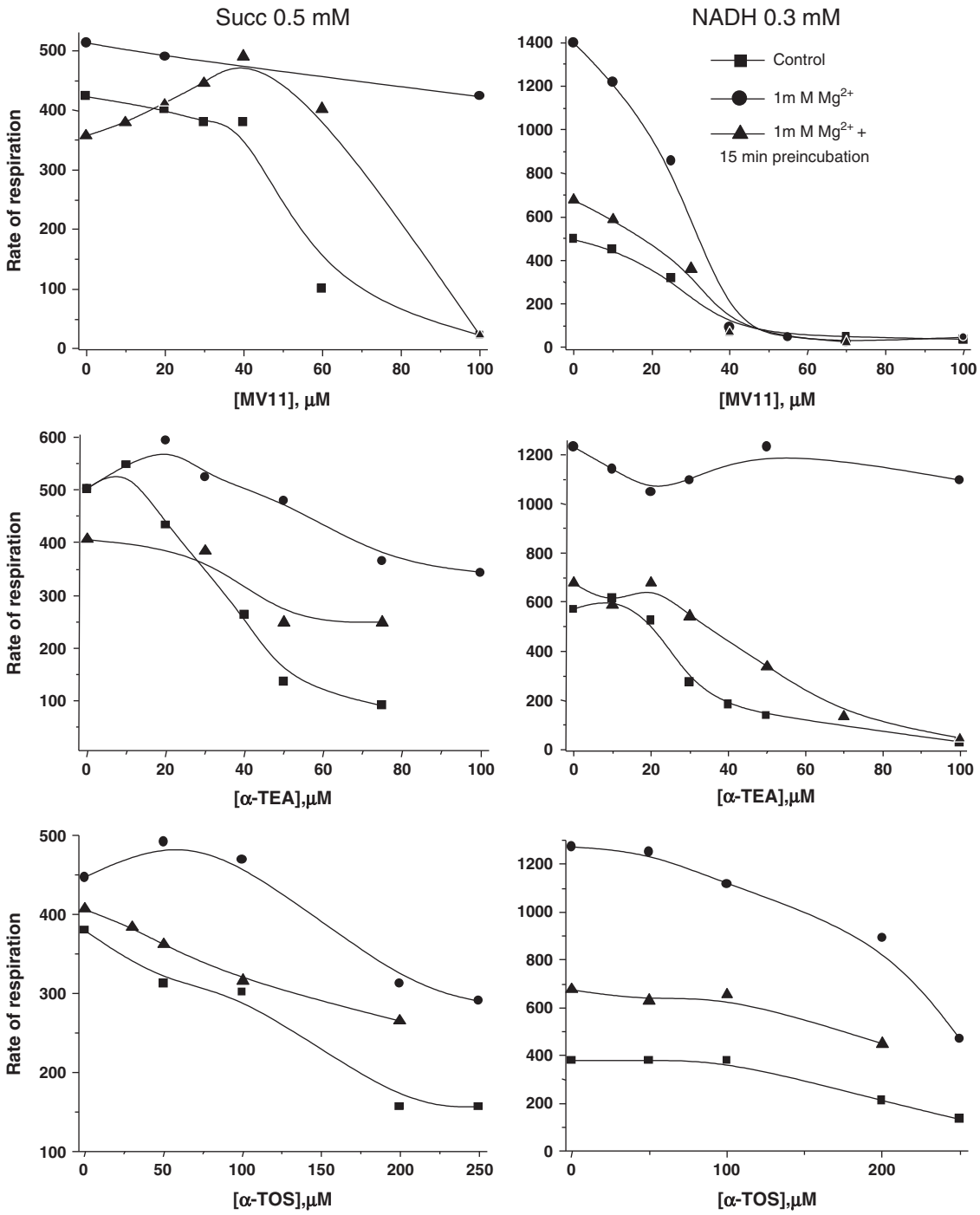

Fig. 6. Effect of vitamin E analogues on SMP respiratory rates. Respiration was determined in the absence (■) or in the presence (●) of 1 mM $MgCl_2$; or after 15 min pre-incubation with drug (▲).

corresponded to the activity of a typical uncoupler (*i.e.*, stimulation of respiration and inhibition of OxPhos, which is equal to the rate of oligomycin-sensitive respiration). Interestingly, the OxPhos rates of AS-30D hepatoma cells and human HeLa carcinoma cells were more sensitive to MitoVES than those of rat hepatocytes (Fig. 8, Table 4), and the agent was effective at relatively lower doses than those required for other anti-cancer drugs acting *via* mitochondria [reviewed in 1]. However, the uncoupling effect induced by 10 μM MitoVES in hepatocytes and HeLa (Figs. 7 and 8) cells was not as potent as that attained with the AS-30D cells. These results (Fig. 8) clearly indicate that the predominant effect of MitoVES at low doses (1–10 μM) in human cancer cells is to lower OxPhos rates by acting as an uncoupler. TTFA (100–250 μM) did not affect the total respiration rates in AS-30D cells but strongly inhibited the oligomycin-sensitive respiration (OXPhos) (data not shown).

High concentrations (200–300 μM) of α-TEA or α-TOS did not show any effects on either the total respiration or OxPhos rates in rat hepatoma or HeLa cells even after incubations for 5–15 min at 37 °C (data not shown).

The $\Delta\psi_m$ was also directly assessed in intact cells following the fluorescence signal of rhodamine 6G [25,26]. To ensure that the signal was reliably monitoring $\Delta\psi_m$ the effect of oligomycin, a specific mitochondrial ATP synthase inhibitor, and the uncoupler CCCP was determined. After reaching a stable signal, the addition of oligomycin

Table 3
Vitamin E analogue IC_{50} (μM) values on respiratory chain complexes in beef heart SMPs.

Compound	Activity	Succ (mM)		NADH (mM)	
		0.25–0.5	2	0.1	1
MitoVES	Dehydrogenase	44 ± 28 (3)	60 ± 20 (3)[a]	> 100 (3)	> 100 (1)
	Oxidoreductase	7.4 ± 5.5 (3)[b]	5.6 ± 5.2 (5)[a,c]	46.7 (2)	> 100 (4)[c]
α-TEA	Dehydrogenase	20 (1)	33.6 (1)	ND	> 250 (1)
	Oxidoreductase	131 ± 23 (3)[b]	37.6 (1)	> 150 (1)	> 100 (2)
α-TOS	Dehydrogenase	39 (2)	32 (1)	> 100 (2)	ND
	Oxidoreductase	> 100(2)	> 100(3)	> 100(1)	> 100 (2)

Dehydrogenase and oxidoreductase activities were determined after 10–15 min incubation with the drugs at 37 °C. Absolute values of dehydrogenase activities were in the range of 70–150 for 0.25–0.5 mM succinate; 90–270 for 2 mM succinate; 355–700 for 0.1 mM NADH; and 744–1100 nmol/min/mg protein for 1 mM NADH, respectively. Absolute values of oxidoreductase activities were 195–400 for 0.25–0.5 mM succinate; 70–350 for 2 mM succinate; 212–418 for 0.1 mM NADH; and 307–1076 nmol/min/mg protein for 1 mM NADH, respectively. Values represent media ± standard deviation; (n); Succ, succinate, ND, not determined. [a,b] $P < 0.005$

induced a further quenching of the probe signal, indicating an increase in $\Delta\psi_m$ because oligomycin fully and specifically blocks OxPhos, the mitochondrial pathway that consumes $\Delta\psi_m$ to synthesize ATP. To specifically and completely collapse the $\Delta\psi_m$, CCCP was added (Fig. 9). The magnitude of the $\Delta\psi_m$ generated by AS-30D cells was appreciably higher than that achieved by rat hepatocytes (136 ± 46 arbitrary fluorescence units (n = 4) *vs.* 68 arbitrary fluorescence units (n = 2) in AS-30D cells and hepatocytes, respectively). The difference in $\Delta\psi_m$ between both types of cells might be attributed to differences in the number of living cells used as the tumor cells showed cell viabilities greater than 95% whereas hepatocytes only were 60–80% viable. However, the magnitude of the $\Delta\psi_m$ in AS-30D cells doubled that in hepatocytes. Similar results have been described by others [36,37; reviewed in 1]. MitoVES at 2 μM induced significant collapse of the $\Delta\psi_m$ in tumor cells but it was innocuous in hepatocytes (Fig. 9). This difference in MitoVES sensitivity between tumor and non-tumor cells was also reproducible at lower cell numbers, but requiring lower MitoVES concentrations (data not shown). TTFA at 10–25 μM induced a less profound partial collapse of the $\Delta\psi_m$ (Fig. 9).

To further assess whether the MitoVES-induced abolishment of OxPhos in cancer cells also leads to significant cellular ATP depletion, compromising cellular homeostasis, the content of cellular ATP was determined. In the presence of the drug at concentrations that severely diminished OxPhos ([MitoVES] > OxPhos IC_{50}), it was found that MitoVES caused substantial lowering of the ATP levels in AS-30D and HeLa cells, and in normal hepatocytes (Table 4). However, in the AS-30D and HeLa cells, the ATP depletion was by 73–81% at 10–11 μM MitoVES, whereas in hepatocytes it decreased by 62–78% at 37 μM MitoVES (see Table 4) in 15–30 min-incubations. Remarkably, at 10 μM MitoVES, the OxPhos rate and ATP content were only slightly altered (~18%) in hepatocytes after 30 min-incubation at 37 °C (Table 4).

Longer-term incubations (60 min) increased the MitoVES efficacy to induce maximal ATP depletion neither in the AS-30D tumor cells (from 10.4 to 2.1 nmol/mg protein; using 11 μM MitoVES) nor in hepatocytes (from 3.6 to 0.6 nmol/mg protein; with 37 μM MitoVES). On the other hand, incubation of HeLa cells for 60 min with 3.5 μM MitoVES caused significant ATP depletion of 47%, contrasting with the negligible drug effect after 15 min incubation (Table 4).

4. Discussion

4.1. Targeting of tumor mitochondria

One of the major problems with current cancer chemotherapeutic treatments is their lack of specificity, leading to multiple severe side-effects. Therefore, it is imperative to develop novel anticancer drugs, which can specifically target malignant cells leaving normal cells unscathed. The promising drugs α-TOS and its derivatives are efficiently hydrolyzed and inactivated by normal cells with high esterase activity, whereas they are not hydrolyzed in cancer cells due to low esterase activity. Moreover, these agents interact with specific cellular targets, leading to apoptosis and death of cancer cells [13,14, reviewed in 16]. Another feature of α-TOS and its derivatives as anti-cancer drugs is their stronger inherent efficacy at acidic pH, which commonly exists in the tumor microenvironment. Most cancer cells exhibit enhanced glycolytic activity and

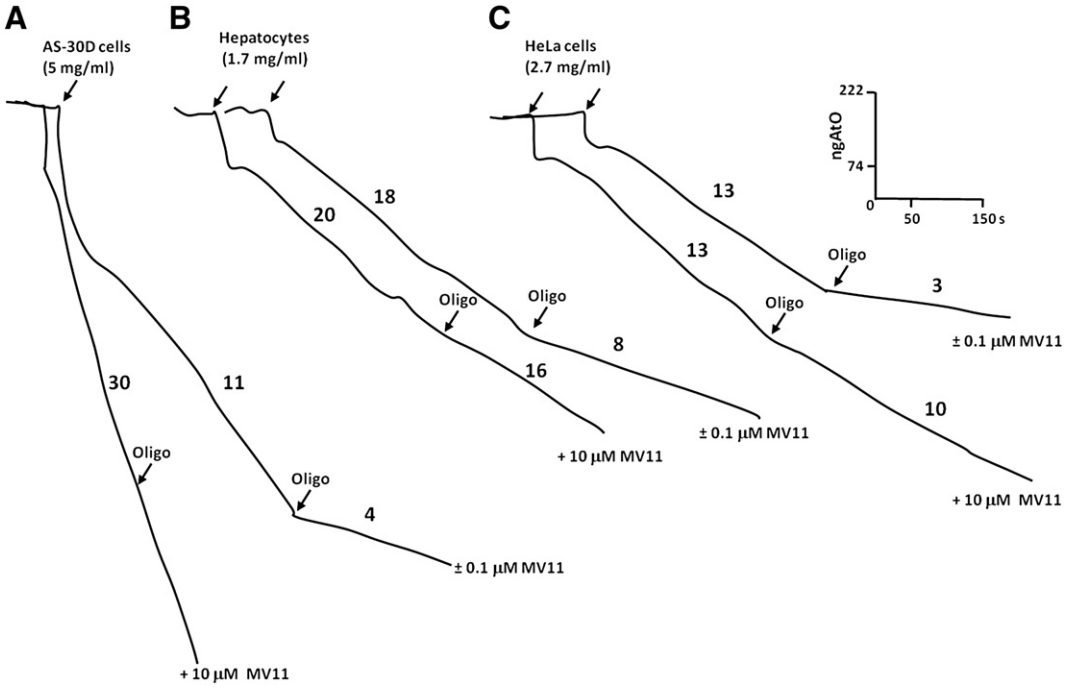

Fig. 7. Cellular respiration of (A) AS-30D hepatoma, (B) rat hepatocyte and (C) HeLa carcinoma cells. Added cellular proteins and MitoVES (MV11) concentrations are indicated. The numbers on the traces indicate the rates of O_2 uptake in nanogram atoms oxygen min^{-1} mg $protein^{-1}$ (ngAtO). Oligo, 5 μM oligomycin.

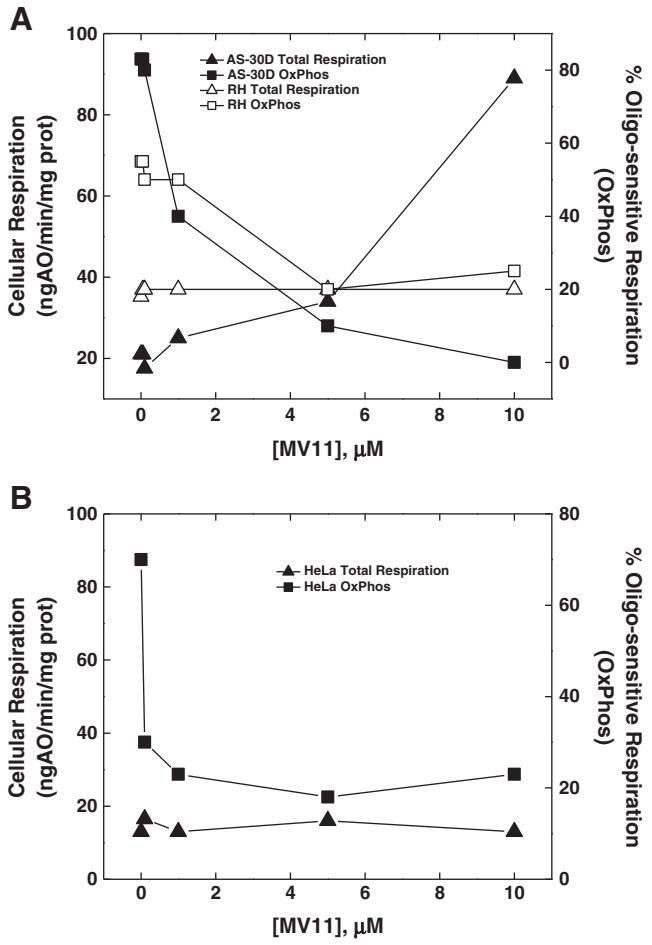

Fig. 8. Effect of MitoVES (MV11) on the rate of cellular respiration and ATP synthesis (oligomycin-sensitive respiration) in (A) AS-30D hepatoma cells and hepatocytes; and (B) in HeLa cells. % Oligo-sensitive respiration in the absence of MitoVES corresponds to 17.5±9 (n=5), 10±6 (n=4) and 13±4 (n=4) nanogram atoms oxygen min^{-1} mg $protein^{-1}$ for AS-30D, hepatocytes and HeLa cells, respectively. The experiment shown is representative of 4–5 independent studies with similar reproducible results.

the end-products of this pathway (lactate, H^+) decrease cytosolic and, in particular extracellular pH as compared to normal cells [reviewed in 38].

Previous efforts to increase targeting of anti-cancer drugs have involved the administration of lipophilic cations. This approach is based on the significantly higher electrical potential across both plasma and inner mitochondrial membranes ($\Delta\psi_p$ and $\Delta\psi_m$, respectively) in cancer cells and mitochondria than in their respective normal counterparts [36,37; reviewed in 1, 39]. Consequently, lipophilic cations are accumulated to a larger extent inside cancer cells and their mitochondria, leading to the collapse of $\Delta\psi_p$ and $\Delta\psi_m$, ATP depletion and cellular death [reviewed in 1]. Hence, the highly lipophilic and delocalized positive charge of MitoVES explains its significantly greater selectivity towards tumor mitochondria [13].

4.2. Efficient mitochondrial uncoupling and moderate CII inhibition by MitoVES

In the 1–10 μM range MitoVES exerted a potent uncoupling effect on both isolated mitochondria and intact hepatoma cells, which resulted in the stimulation of basal (state 4 and pseudo state 4) respiration and ATP hydrolysis, and inhibition of mitochondrial ATP synthesis (*c.f.* Figs. 2 and 8A). To unambiguously establish whether MitoVES behaved as an uncoupler, other energy-dependent parameters were assessed in isolated mitochondria. Membrane potential and Ca^{2+} release were more sensitive mitochondrial parameters than respiration and ATP hydrolysis for detecting the MitoVES uncoupling effect, regarding response times and the doses required. At the same 1–10 μM range, MitoVES diminished $\Delta\psi_m$ and induced Ca^{2+} release of tumor and normal mitochondria (*c.f.* Figs. 3–5), as do classical uncouplers [40,41].

The inhibition of net state 3 respiration in mitochondria by low MitoVES (*c.f.* Fig. 2C; Table 3) correlated with lowering of the tumor cell OxPhos (*c.f.* Fig. 8). Indeed, OxPhos of both human HeLa carcinoma and rodent AS-30D hepatoma cells was affected (Fig. 8) at relatively low MitoVES levels (1–3 μM; Table 3), while the MitoVES IC_{50} for net state 3 respiration in hepatoma mitochondria was 1.6 μM (Table 2). However, at 1–3 μM MitoVES, the ATP levels were only slightly affected (Table 4), indicating the onset of compensatory mechanisms that preserve the cellular ATP homeostasis, possibly glycolysis activation and decreased ATP demand. On the other hand, at 10–11 μM MitoVES sufficed to induce severe cellular ATP depletion in tumor cells, compromising cellular integrity (*c.f.* Table 4).

Conceivably, several lipophilic drugs with delocalized net positive charge (clotrimazole, rhodamine 123, MKT-077) and the DNA-intercalators benzophenone guttiferone-A [42] and doxorubicin [43], may also significantly impair the mitochondrial function

Table 4
MitoVES effect on OxPhos and ATP content in normal and tumor cells.

	OxPhos IC_{50} (μM), 2–15-min incubation	ATP content (nmol/mg protein)		
		Control	+[MitoVES]	
Rat				
AS-30D Hepatoma	1.4±1 (5)	15-min incubation: 10.4±3.3 (5)	8.5 (2)+[3.5 μM]	1.9±0.4 (3)[a]+[11 μM]
		30-min incubation: 10.5±3.9 (5)	9.7 (2)+[3.5 μM]	2±0.6 (3)[b]+[11 μM]
Hepatocytes	61±9 (4)	15-min incubation: 5.2±0.8 (6)	3.6±0.5 (4)[b]+[10 μM]	2±0.6 (3)[a]+[37 μM]
		30-min incubation: 4.6±0.5 (4)	3.8±0.2 (4)[c]+[10 μM]	1±0.5 (3)[a]+[37 μM]
Human				
Cervix HeLa	3.5±0.7 (3)	15-min incubation: 4.4±2.2 (6)	4±3 (3)+[3.5 μM]	2.1±1.1 (3)[d]+[10 μM]
		30-min incubation: 4.6±2.1 (7)	4.1±3.1 (4)+[3.5 μM]	2.3±1 (3)+[10 μM]
		60-min incubation: 4.2±1.2 (6)	2.3±1 (3)[d]+[3.5 μM]	1.7±0.7 (3)[c]+[10 μM]

Rat hepatocytes (35 μM), rat hepatoma (11 μM) and human tumor cells (3.5 μM) were incubated with variable concentrations of MitoVES for the indicated times at 37 °C. Total OxPhos values were 15±9 (5); 12±6 (4); and 10±6 (6) ngAO/min/mg protein for AS-30D hepatoma, HeLa and rat hepatocytes, respectively. For a different second MitoVES batch, OxPhos IC_{50} was 11±4 (n=4) in hepatoma cells. Because of the experimental variability observed when taking all values into account (IC_{50}=6.3±6, n=9), the results obtained with the first MitoVES batch were only included in the table. Values represent media±standard deviation, with the number of different preparations assayed between parentheses.

[a] P<0.005 *versus* control.
[b] P<0.01.
[c] P<0.025.
[d] P<0.05.

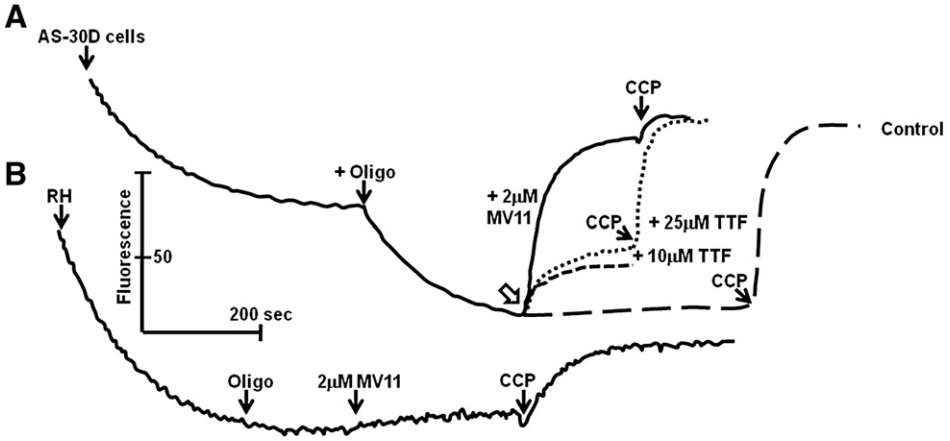

Fig. 9. Mitochondrial electrical membrane potential in AS-30D hepatoma cells (A) and rat hepatocytes (B). The change in the fluorescence signal of rhodamine 6G was determined as described under Material and methods. Open block arrow indicates the addition of either MV11 or TTFA (TTF). Abbreviations: CCP, 5 μM CCCP; MV11, MitoVES; Oligo, 5 μM oligomycin; RH, rat hepatocytes. The experiments shown are representative of 4 and 2 independent AS-30D cell and hepatocytes preparations, respectively, with similar reproducible results.

(mitochondrial hexokinase detachment; cytochrome *c* oxidase, ATP synthase and ANT inhibition; mtDNA decrease) in tumor mitochondria. However, the doses required for the activity of these antineoplastic drugs are 7–10 times higher than those required for MitoVES to affect the mitochondrial bioenergetics of cancer cells [reviewed in 1,44,45]. Therefore, MitoVES is an attractive drug for the use in clinical trials given its activity at relatively low concentrations and its apparently negligible side-effects [13]. Furthermore, low MitoVES concentrations that drastically decrease OxPhos also cause substantial growth suppression in aggressive, fast-growing carcinomas with IC_{50} values of 3.9 μM, 20 μM and 15 μM after 24 h for HeLa, breast MCF-7 and prostate PC3 cells, respectively. This indicates that mitochondria-targeted drugs epitomized by MitoVES show a considerable potential to control metastatic and aggressive behavior of cancer cells.

Recent reports [12,13,44] have documented that the preferred target for the action of MitoVES in cancer cells is the respiratory CII. To further extend this observation, the effects of α-TOS and α-TEA on the dehydrogenase and oxidoreductase activities of CII in SMPs were compared to those of MitoVES. As the control, the dehydrogenase and oxidoreductase activities of CI were also examined.

The CII oxidoreductase activity was significantly more sensitive to MitoVES than the dehydrogenase activity (*c.f.* Table 3). The effect of MitoVES on CII involves interactions of the succinyl-tocopheryl moiety of the agent with the ubiquinone binding site of CII [13], as shown earlier also for the less efficient α-TOS [14]. Therefore, MitoVES may differentially affect the two CII activities. Indeed, kinetic analysis of the type of inhibition of the CII oxidoreductase activity by MitoVES yielded a complex pattern characterized by mixed inhibition at concentrations < 50 μM and uncompetitive inhibition at 50–200 μM (data not shown). The CI dehydrogenase and oxidoreductase activities were unaffected by 100 μM or lower MitoVES concentrations (*c.f.* Table 3). These results clearly established that MitoVES preferentially associates with CII and not with CI or CIII [12,13]. Moreover, it has been recently documented that the interaction of MitoVES specifically with CII induces ROS production and apoptosis within relatively short times in several different cancer cell lines [13,44].

The TPP^+-lacking α-TOS and α-TEA were also effective in inhibiting CII activities, albeit to a lesser extent. However, it should be noted that in SMPs, the succinate binding site is freely accessible (*i.e.*, the drugs do not need to traverse the hydrophobic core of the inner mitochondrial membrane to interact with CII) and therefore the reason why these drugs were less potent than MitoVES in intact mitochondria is probably due to their lower permeability across the inner membrane. This issue still needs to be resolved.

MitoVES was found more efficient than α-TOS or α-TEA at inducing mitochondrial dysfunction in intact cells. In fact, α-TOS and α-TEA at 100–300 μM did not affect the respiratory rates and OxPhos in hepatocytes and hepatoma cells (*c.f.* Tables 1, 2 and 4). This observation correlates with the relatively low efficacy of α-TOS to induce apoptosis in Jurkat cells compared to MitoVES (MitoVES is 1–2 orders of magnitude more apoptogenic than α-TOS) [13,44]. A possible explanation for these differences may be that cancer mitochondria *in situ* maintain greater $\Delta\psi_m$ than normal mitochondria [reviewed in 1], and this drives the lipophilic cationic MitoVES to penetrate and accumulate at the inter-phase of the mitochondrial matrix and the inner membrane [13,44], whereas α-TOS and α-TEA with no net positive charge associate indiscriminately with cellular hydrophobic structures. Preferential distribution at the mitochondrial matrix–inner membrane inter-phase has also been reported for mitochondrially targeted redox-active compounds, the prime example being the mitochondrially targeted coenzyme Q (MitoQ) [45,46].

Isolated tumor mitochondria and tumor cells were 2–7 and 3–10 times, respectively, more sensitive to the MitoVES effects (when uncoupling and inhibiting OxPhos) than normal mitochondria and cells (*c.f.* Figs. 2 and 8 and Tables 1, 2 and 4), indicating exceptionally high cancer cell selectivity of MitoVES. This highly intriguing feature of MitoVES has also been documented when analyzing its effects on the growth of several different cancer cell lines and on the kinetics of progression of tumors in mouse models [12,13,44]. The molecular mechanism of the selectivity of the drug for malignant cells also involves the inherently higher esterase activity in normal cells *versus* the low or negligible activity found in cancer cells [47], since the esterase in normal cells releases the succinyl moiety of the VE ester analogues, thwarting their anchoring ability to combine with and inhibit CII.

In conclusion, the results presented in this work support the following sequence of events for MitoVES action on cancer cells and their mitochondria. At low doses (1–10 μM), increased uptake of MitoVES promotes $\Delta\psi_m$ dissipation which in turn inhibits OxPhos and stimulates O_2 consumption, leading to ATP depletion. At moderate doses of 10–20 μM, MitoVES inhibits the oxidoreductase activity of CII, while at 40–60 μM, the dehydrogenase CII activity is inhibited; CI and CIII activities are inhibited at substantially higher MitoVES concentrations. Inhibition of CII activity by MitoVES brings about the additional deleterious effect of increasing ROS production. Collectively, our findings strongly point to the mitochondrially targeted VE analogue MitoVES as a suitable and highly promising candidate for cancer therapy, acting in a multi-task manner and being highly selective for cancer cell mitochondria [1–14,44].

Acknowledgements

The present work was partially supported by grants from CONACyT-México (nos. 80534, 107183 and 123636) and Instituto de Ciencia y Tecnología del Distrito Federal (no. PICS08-5) to RMS and SRE. ETA was supported in part by grants from the NIH (5R01CA120552) and the Australian–American Fulbright Commission. JN was supported in part by grants from the Australian Research Council and the Czech Scientific Foundation (P301/10/1937).

Appendix A. Supplementary data

Supplementary data to this article can be found online at http://dx.doi.org/10.1016/j.bbabio.2012.05.005.

References

[1] S. Rodríguez-Enríquez, A. Marín-Hernández, J.C. Gallardo-Pérez, L. Carreño-Fuentes, R. Moreno-Sánchez, Targeting of cancer energy metabolism, Mol. Nutr. Food Res. 53 (2009) 29–48.
[2] J. Rohlena, L.F. Dong, S.J. Ralph, J. Neuzil, Anti-cancer drugs targeting the mitochondrial electron redox chain, Antioxid. Redox Signal. 15 (2011) 2951–2974.
[3] P. Horak, A.R. Crawford, D.D. Vadysirisack, Z.M. Nash, M.P. DeYoung, D. Sgroi, L.W. Ellisen, Negative feedback control of HIF-1 through REDD1-regulated ROS suppresses tumorigenesis, Proc. Natl. Acad. Sci. U. S. A. 107 (2010) 4675–4680.
[4] S.J. Ralph, S. Rodríguez-Enríquez, J. Neuzil, E. Saavedra, R. Moreno-Sánchez, The causes of cancer revisited: hypoxia and glucose deprivation drive mitochondrial ROS induced oncogenic mutation and malignant transformation—implication for the selective targeting of cancer therapy, Mol. Aspects Med. 31 (2010) 145–170.
[5] L.R. Cavalli, B.C. Liang, Mutagenesis, tumorigenicity, and apoptosis: are the mitochondria involved? Mutat. Res. 398 (1998) 19–26.
[6] J.S. Penta, F.M. Johnson, J.T. Wachsman, W.C. Copeland, Mitochondrial DNA in human malignancy, Mutat. Res. 488 (2001) 119–133.
[7] T. Murata, H. Hibasami, S. Maekawa, T. Tagawa, K. Nakashima, Preferential binding of cisplatin to mitochondrial DNA and suppression of ATP generation in human malignant melanoma cells, Biochem. Int. 20 (1990) 949–955.
[8] O.A. Olivero, C. Semino, A. Kassim, D.M. Lopez-Larraza, M.C. Poirer, Preferential binding of cisplatin to mitochondrial DNA of Chinese hamster ovary cells, Mutat. Res. 346 (1995) 221–230.
[9] D.A. Clayton, J.N. Doda, E.C. Friedberg, The absence of a pyrimidine dimer repair mechanism in mammalian mitochondria, Proc. Natl. Acad. Sci. U. S. A. 71 (1974) 2777–2781.
[10] G. Ara, T. Kusumoto, T.T. Korbut, F. Cullere-Luengo, B.A. Teicher, Cisdiamminedichloroplatinum (II) resistant human tumor cell lines are collaterally sensitive to PtCl4 (RH-123) 2: evidence for mitochondrial involvement, Cancer Res. 54 (1994) 1497–1502.
[11] J. Neuzil, T. Weber, N. Gellert, C. Weber, Selective cancer cell killing by a-tocopheryl succinate, Br. J. Cancer 84 (2001) 87–89.
[12] L.F. Dong, R. Freeman, J. Liu, R. Zobalova, A. Marín-Hernández, M. Stantic, J. Rohlena, S. Rodríguez-Enríquez, K. Valis, B. Butcher, J. Goodwin, U.T. Brunk, P.K. Witting, R. Moreno-Sánchez, I.E. Scheffler, S.J. Ralph, J. Neuzil, Suppression of tumour growth *in vivo* by the mitocan α-TOS requires respiratory complex II, Clin. Cancer Res. 15 (2009) 1593–1600.
[13] L.F. Dong, V.J. Jameson, D. Tilly, J. Cerny, E. Mahdavian, A. Marín-Hernández, L. Hernández-Esquivel, S. Rodríguez-Enríquez, J. Stursa, P.K. Witting, B. Stantic, J. Rohlena, J. Truksa, K. Kluckova, J.C. Dyason, M. Ledvina, B.A. Salvatore, R. Moreno-Sánchez, M.J. Coster, S.J. Ralph, R.A. Smith, J. Neuzil, Mitochondrial targeting of vitamin E succinate enhances its pro-apoptotic and anti-cancer activity via mitochondrial complex II, J. Biol. Chem. 286 (2011) 3717–3728.
[14] L.F. Dong, P. Low, J.C. Dyason, X.F. Wang, L. Prochazka, P.K. Witting, R. Freeman, E. Swettenham, K. Valis, J. Liu, R. Zobalova, J. Turanek, D.R. Spitz, F.E. Domann, I.E. Scheffler, S.J. Ralph, J. Neuzil, α-Tocopheryl succinate induces apoptosis by targeting ubiquinone-binding sites in mitochondrial respiratory complex II, Oncogene 27 (2008) 4324–4335.
[15] C.W. Shiau, J.W. Huang, D.S. Wang, J.R. Weng, C.C. Yang, C.H. Lin, C. Li, C.S. Chen, α-Tocopheryl succinate induces apoptosis in prostate cancer cells in part through inhibition of Bcl-x_L/Bcl-2 function, J. Biol. Chem. 281 (2006) 11819–11825.
[16] S.J. Ralph, R. Moreno-Sánchez, R. Neuzil, S. Rodríguez-Enríquez, Inhibitors of succinate:quinone reductase/complex II regulating production of mitochondrial reactive oxygen species protect normal cells from ischemic damage but cause cancer cell death, Pharm. Res. 112 (2011) 2703–2715.
[17] C. Beltrán, M. Tuena de Gómez-Puyou, A. Gómez-Puyou, A. Darszon, Release of the inhibitory action of the natural ATPase inhibitor protein on the mitochondrial ATPase, Eur. J. Biochem. 144 (1984) 151–157.
[18] R. Moreno-Sánchez, Regulation of oxidative phosphorylation in mitochondria by external free Ca^{+2} concentrations, J. Biol. Chem. 260 (1985) 4028–4034.
[19] F. López-Gómez, M.E. Torres-Márquez, R. Moreno-Sánchez, Control of oxidative phosphorylation in AS-30D hepatoma mitochondria, Int. J. Biochem. 25 (1993) 373–377.
[20] S. Rodríguez-Enríquez, M.E. Torres-Márquez, R. Moreno-Sánchez, Substrate oxidation and ATP supply in AS-30D hepatoma cells, Arch. Med. Res. 29 (2000) 1–12.
[21] S. Rodríguez-Enríquez, P.A. Vital-González, F.L. Flores-Rodríguez, A. Marín-Hernández, L. Ruiz-Azuara, R. Moreno-Sánchez, Control of cellular proliferation by modulation of oxidative phosphorylation in human and rodent fast-growing tumor cells, Toxicol. Appl. Pharmacol. 215 (2006) 208–217.
[22] M.N. Berry, D.S. Friend, High-yield preparation of isolated rat liver parenchymal cells. A biochemical and fine structural study, J. Cell Biol. 43 (1969) 506–520.
[23] A. Atlante, S. Passarella, P. Pierro, C. Di Martino, E. Quagliariello, The mechanism of proline/glutamate antiport in rat kidney mitochondria. Energy dependence and glutamate-carrier involvement, Eur. J. Biochem. 241 (1996) 171–177.
[24] H. Rottenberg, R. Moreno-Sánchez, The proton pumping activity of H(+)-ATPases: an improved fluorescence assay, Biochim. Biophys. Acta 1183 (1993) 161–170.
[25] M. Mandalá, G. Serck-Hanssen, G. Martino, K.B. Helle, The fluorescent cationic dye rhodamine 6G as a probe for membrane potential in bovine aortic endothelial cells, Anal. Biochem. 274 (1999) 1–6.
[26] L.V. Johnson, M.L. Walsh, B.J. Bockis, L.B. Chen, Monitoring of relative mitochondrial membrane potential in living cells by fluorescence microscopy, J. Cell Biol. 88 (1981) 526–535.
[27] F. Pacheco-Moisés, J.J. García, J.S. Rodríguez-Zavala, R. Moreno-Sánchez, Sulfite and membrane energization induce two different active states of the *Paracoccus denitrificans* F0F1-ATPase, Eur. J. Biochem. 267 (2000) 993–1000.
[28] M. Nishimura, T. Ito, B. Chance, Studies on bacterial phosphorylation. III. A sensitive and rapid method of determination of photophosphorylation, Biochim. Biophys. Acta 59 (1962) 177–182.
[29] R. Moreno-Sánchez, C. Bravo, J. Gutierrez, A.H. Newman, P.K. Chiang, Release of Ca^{2+} from heart and kidney mitochondria by peripheral-type benzodiazepine receptor ligands, Int. J. Biochem. 23 (1991) 207–213.
[30] J.M. Armstrong, The molar extinction coefficient of 2,6 dichlorophenol indophenols, Biochim. Biophys. Acta 86 (1964) 194–197.
[31] R. Covián, R. Moreno-Sánchez, Role of protonatable groups of bovine heart bc1 complex in ubiquinol binding and oxidation, Eur. J. Biochem. 268 (2001) 5783–5790.
[32] H.U. Bergmeyer, Metabolites 1, carbohydrates, in: H.U. Bergmeyer (Ed.), Methods of Enzymatic Analysis, Weinheim Verlag Chemie, Germany, 1983.
[33] C.A. Yu, L. Yu, T.E. King, Reconstitution of succinate-Q reductase, Biochem. Biophys. Res. Commun. 79 (1977) 939–946.
[34] B.L. Trumpower, Z. Simmons, Diminished inhibition of mitochondrial electron transfer from succinate to cytochrome *c* by thenoyltrifluoroacetone induced by antimycin, J. Biol. Chem. 176 (1979) 4608–4616.
[35] R.F. Thorne, F.L. Bygrave, Energy-linked functions of tightly coupled mitochondria isolated from Ehrlich acsites tumor cells, Cancer Res. 33 (1973) 2562–2567.
[36] J.S. Modica-Napolitano, J.R. Aprille, Basis for the selective cytotoxicity of rhodamine 123, Cancer Res. 47 (1987) 4361–4365.
[37] S. Davis, M.J. Weiss, J.R. Wong, T.J. Lampidis, L.B. Chen, Mitochondrial and plasma membrane potentials cause unusual accumulation and retention of rhodamine 123 by human breast adenocarcinoma-derived MCF-7 cells, J. Biol. Chem. 260 (1985) 13844–13850.
[38] R. Moreno-Sánchez, S. Rodríguez-Enríquez, A. Marín-Hernández, E. Saavedra, Energy metabolism in tumor cells, FEBS J. 273 (2007) 5703–5713.
[39] V.R. Fantin, M.J. Berardi, L. Scorrano, S.J. Korsmeyer, P. Leder, A novel mitochondriotoxic small molecule that selectively inhibits tumor cell growth, Cancer Cell 2 (2002) 29–42.
[40] V.P. Skulachev, Uncoupling: new approaches to an old problem of bioenergetics, Biochim. Biophys. Acta 1363 (1998) 125–133.
[41] S. Miwa, M.D. Brand, Mitochondrial matrix reactive oxygen species production is very sensitive to mild uncoupling, Biochem. Soc. Trans. 31 (2003) 1300–1301.
[42] G.L. Pardo-Andreu, Y. Nuñez-Figueredo, V.G. Tudella, O. Cuesta-Rubio, F.P. Rodrigues, C.R. Pestana, S.A. Uyemura, A.M. Leopoldino, L.C. Alberici, C. Curti, The anti-cancer agent guttiferone-A permeabilizes mitochondrial membrane: ensuing energetic and oxidative stress implications, Toxicol. Appl. Pharmacol. 253 (2011) 282–289.
[43] A.V. Kuznetsov, R. Margreiter, A. Amberger, V. Saks, M. Grimm, Changes in mitochondrial redox state, membrane potential and calcium precede mitochondrial dysfunction in doxorubicin-induced cell death, Biochim. Biophys. Acta 1813 (2011) 1144–1152.
[44] L.F. Dong, V.J.A. Jameson, D. Tilly, L. Prochazka, J. Rohlena, K. Valis, J. Truksa, R. Zobalova, E. Mahdavian, K. Kluckova, M. Stantic, J. Stursa, X.F. Wang, R. Freeman, P.K. Witting, E. Norberg, J. Goodwin, B.A. Salvatore, J. Novotna, J. Turanek, M. Ledvina, P. Hozak, B. Zhivotovsky, M.J. Coster, S.J. Ralph, R.A.J. Smith, J. Neuzil, Mitochondrial targeting of α-tocopheryl succinate enhances its pro-apoptotic efficacy: a new paradigm of efficient anti-cancer therapy, Free Radic. Biol. Med. 50 (2011) 1546–1555.
[45] M.P. Murphy, R.A. Smith, Targeting antioxidants to mitochondria by conjugation to lipophilic cations, Annu. Rev. Pharmacol. Toxicol. 47 (2007) 629–656.
[46] R.A. Smith, R.C. Hartley, M.P. Murphy, Mitochondria-targeted small molecule therapeutics and probes, Antioxid. Redox Signal. 15 (2011) 3021–3038.
[47] F. Liewald, N. Demmel, R. Wirsching, H. Kahle, G. Valet, Intracellular pH, esterase activity, and DNA measurements of human lung carcinomas by flow cytometry, Cytometry 11 (1990) 341–348.